Supporting Information

Proton conductivity and dielectric anomalies in a chain-based metal-organic framework with a hydrogen-bonded network of [SO_3] groups, pyrazine and water molecules

Jiechen He,[a]‡ Feirong Chen,[a]‡ Chenxin Lin,[a] Yaozong Chen,[a] Lizhen Liu,*[a] and Zizhu Yao*[b]

a. Key Laboratory of Polymer Materials and Products of Universities in Fujian, Department of Materials Science and Engineering, Fujian University of Technology, Fuzhou 350118, P. R. China;
E-mail: liulizhen@fjut.edu.cn;

b. Fujian Provincial Key Laboratory of Polymer Materials, College of Chemistry and Materials Science, Fujian Normal University, Fuzhou 350007, P. R. China;
E-mail: yaozizhu@fjnu.edu.cn;

‡These authors contributed equally to this work.

Materials and Methods

All reagents and solvents used in synthetic studies are commercially available and were used as supplied without further purification. Powder X-ray diffraction (PXRD) was carried out with a Bruker powder diffractometer equipped with a Cu sealed tube (λ = 1.541874 Å) at 40 kV and 40 mA over the 2θ range of 5-30°. The simulated pattern was produced using the Mercury V1.4 program and single-crystal diffraction data. FT-IR spectra of the synthesized complexes were carried out on a Nicolet 5700 FT-IR spectrometer as KBr pellets. Thermal analysis was carried out on a NETZSCH thermal analyzer from 30 to 600 °C at a heating rate of 10 °C min^{-1} under N_2 flow.

Synthesis of FUT-3. A mixture of 0.169 g $Cu(NO_3)_2 \cdot 6H_2O$ (0.7 mmol), 0.232 g disodium 2,7-Naphthalenedisulfonate ($NDSNa_2$, 0.7 mmol) and 0.056 g pyrazine (0.7 mmol) were dissolved in 5 mL deionized water. The resulting solution was kept at 80 °C for 12h and then cooled to room temperature. Blue needle-shaped crystals were obtained with a yield of ~75% based on Cu^{II}. IR (cm^{-1}): 3446 (m), 3110 (w), 1658 (w),

1413 (m), 1226 (s), 1101 (m), 1029 (s), 796 (m), 705 (s), 576 (m), 493 (w).

Crystallographic Studies

Data collection and structural analysis of **FUT-3** were performed on an Agilent Technologies SuperNova single crystal diffractometer equipped with graphite monochromatic Cu Ka radiation (λ = 1.54184 Å). The crystal was kept at 291(3) K during data collection. Using Olex2[1], the structure was solved with the ShelXT[2] structure solution program using intrinsic phasing approach and refined with the ShelXL[3] refinement package using least squares minimization. The initial indexing results indicated that some diffraction spots displayed elongated or split morphologies, suggesting the possible presence of crystal twinning. A twin law was derived using the twinning module within the CrysAlisPro software. The module analyzes the geometry of the diffraction pattern to identify the orientation relationship between the twin domains. The twin law corresponding to a -179.7456° rotation around the axis [0.9988, 0.0010, -0.0499], expressed as a transformation matrix (TL), was determined as [0.9971 0.0203 0.0005 / 0.0020 -1.0020 0.0007 / -0.0996 -0.0189 -1.0004]. The twin component ratio was refined to 0.212(5). All nonhydrogen atoms were refined with anisotropic displacement parameters. The hydrogen atoms on the ligands were placed at idealized positions and refined using a riding model. The detailed crystallographic data and structure refinement parameters for these compounds are summarized in Table S1 (CCDC: 2497464)

Proton conductivity measurement

Proton conductivity testing was carried out on pelletized samples pressed in a cylindrical die (0.25 cm diameter, 0.35 cm length) at ~0.2 t for 3 minutes to prevent sample decomposition from the high pressure. Impedance analysis was performed on the pellets using a twoprobe method with a Solartron SI 1260 Impedance/GainPhase Analyzer and 1296 Dielectric Interface Impedance Analyzer from 10 MHz to 100 Hz with an input voltage 100 mV. Humidity and temperature were controlled by using a XKCTS80Z humidity control chamber. Measurements were performed at thermal equilibrium by holding for 30 minutes at each measuring temperature. Proton

conductivity was calculated using the following equation:

$$\sigma=\frac{l}{SR} \qquad (1)$$

Where l and S are the length (cm) and cross-sectional area (cm^2) of the samples, respectively, and R, which was extracted directly from the impedance plots, is the bulk resistance of the sample (Ω). Activation energy (E_a) for the material conductivity was estimated from the following equation:

$$\sigma T=\sigma_0 \exp(-\frac{E_a}{k_B T}) \qquad (2)$$

Where σ is the proton conductivity, σ_0 is the preexponential factor, k_B is the Boltzmann constant, and T is the temperature.

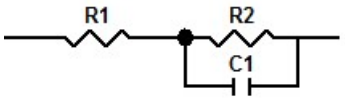

(3)

ZView software was used to extrapolate impedance data results by means of an equivalent circuit simulation (3) to complete the Nyquist plot and obtain the resistance values.

Dielectric measurements

The samples are pressed under pressure (4 MPa) into a small cylinder with a diameter of 6 mm and a thickness of 0.7 mm. Then, the cylinders are coated with a silver paste to produce electrical contacts. All measurements were performed in the frequency range of 100 kHz~2MHz. The dielectric constant and dielectric loss data are measured with constant temperature connected to TongHui 2838 LCR meter. The real part of dielectric constant (ε′) and the imaginary part of the dielectric constant (ε″) were determined by using the following equations:

$$\varepsilon' = \frac{Ct}{\varepsilon_0 A} \qquad (1)$$

$$\varepsilon'' = \varepsilon' \tan\delta \qquad (2)$$

C is the capacitance (F), A is the cross-sectional area of the electrode, and t is the thickness of the sample (cm), ε_0 is the dielectric constant in vacuum ($\varepsilon_0 = 8.854 \times 10^{-14}$ F/cm) and tan δ is the loss tangent.

Table S1 Crystal data and refinement results for the as-synthesized samples.

Identification code	**FUT-3**
CCDC	2497464
Empirical formula	$C_{18}H_{26}CuN_4O_{12}S_2$
Formula weight	618.09
Temperature/K	291(3)
Crystal system	monoclinic
Space group	*P2/c*
a/Å	27.393(2)
b/Å	6.8540(5)
c/Å	13.3403(10)
α/°	90
β/°	91.411(9)
γ/°	90
V/Å^3	2498.9(4)
Z	4
ρ_{calc}g/cm^3	1.643
μ/mm^{-1}	3.423
F(000)	1276.0
Radiation	Cu Kα (λ = 1.54184)
Data/restraints/parameters	6289/4/353
Goodness-of-fit on F^2	1.115
Final R indexes [I>=2σ (I)][a]	R_1 = 0.0915,
	wR_2 = 0.2747
Final R indexes [all data][a]	R_1 = 0.1357,
	wR_2 = 0.3257

[a]$R_1 = \sum(|F_o| - |F_c|) / \sum|F_o|$, [b]$wR_2 = [\sum w(F_o^2 - F_c^2)^2 / \sum w(F_o^2)^2]^{0.5}$

Table S2 Selected bond lengths and bond angle for **FUT-3**.

Atom-Atom	**Length/Å**	**Atom-Atom**	**Length/Å**
Cu2-N3	2.004(15)	Cu1-O2W^3	2.154(10)
Cu2-N4	2.033(17)	Cu1-O1W^3	2.090(11)
Cu2-O4W^1	2.038(10)	Cu1-O1W	2.090(11)
Cu2-O4W	2.038(10)	Cu1-N1	2.073(16)
Cu2-O3W	2.216(10)	Cu1-N2^4	2.013(15)
Cu2-O3W^1	2.216(10)	N2-Cu1^2	2.013(15)
Cu1-O2W	2.154(10)		
Atom-Atom-Atom	**Angle/°**	**Atom-Atom-Atom**	**Angle/°**
N3-Cu2-N4	180.0	N3-Cu2-O4W^1	89.9(3)
N3-Cu2-O4W^1	89.9(3)	N3-Cu2-O3W^1	89.8(3)
N3-Cu2-O3W	89.8(3)	N4-Cu2-O4W	90.1(3)

N4-Cu2-O4W[1]	90.1(3)	N4-Cu2-O3W	90.2(3)
N4-Cu2-O3W[1]	90.2(3)	O4W-Cu2-O4W[1]	179.7(6)
O4W-Cu2-O3W	90.9(5)	O4W[1]-Cu2-O3W[1]	90.9(5)
O4W-Cu2-O3W[1]	89.1(5)	O4W[1]-Cu2-O3W	89.1(5)
O3W-Cu2-O3W[1]	179.6(5)	O2W-Cu1-O2W[3]	179.7(6)
O1W[3]-Cu1-O2W	91.4(4)	O1W-Cu1-O2W	88.5(4)
O1W-Cu1-O2W[3]	91.4(4)	O1W[3]-Cu1-O2W[3]	88.5(4)
O1W-Cu1-O1W[3]	179.0(7)	N1-Cu1-O2W[3]	89.8(3)
N1-Cu1-O2W	89.8(3)	N1-Cu1-O1W	89.5(4)
N1-Cu1-O1W[3]	89.5(4)	N2[4]-Cu1-O2W	90.2(3)
N2[4]-Cu1-O2W[3]	90.2(3)	N2[4]-Cu1-O1W	90.5(4)
N2[4]-Cu1-O1W[3]	90.5(4)	N2[4]-Cu1-N1	180.0

[1]-X,+Y,-1/2-Z; [2]+X,-1+Y,+Z;; [3]1-X,+Y,1/2-Z; [4]+X,1+Y,+Z

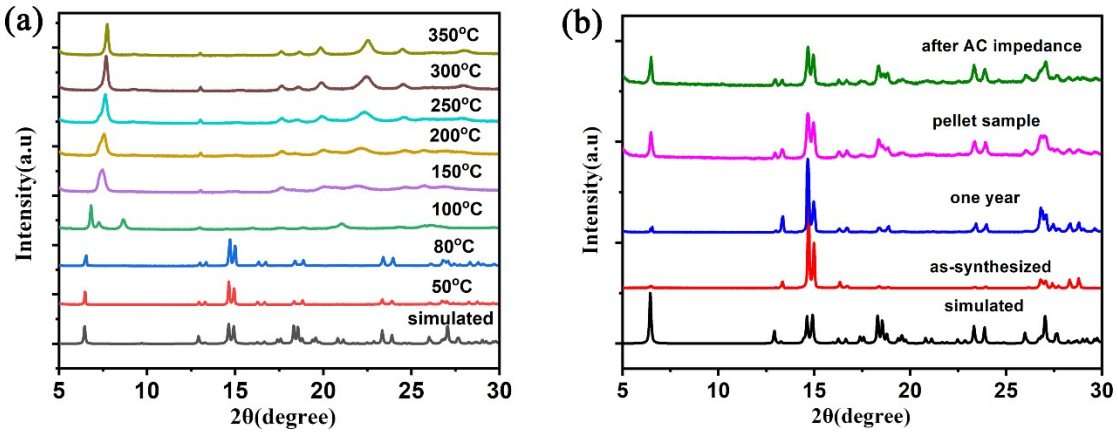

Fig. S1 PXRD patterns of **FUT-3** treated with at different temperature (a) and different condition (b).

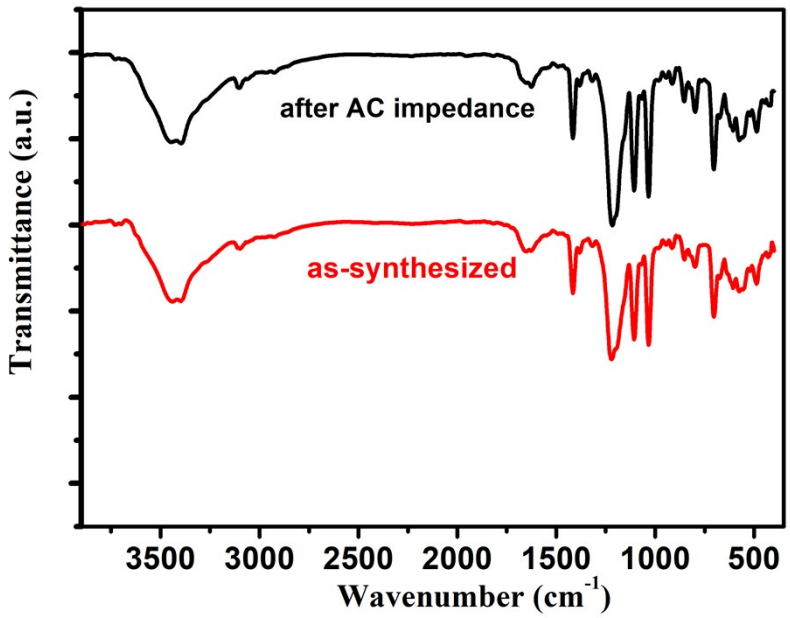

Fig. S2 IR spectra of as-synthesized and after AC impedance in **FUT-3**.

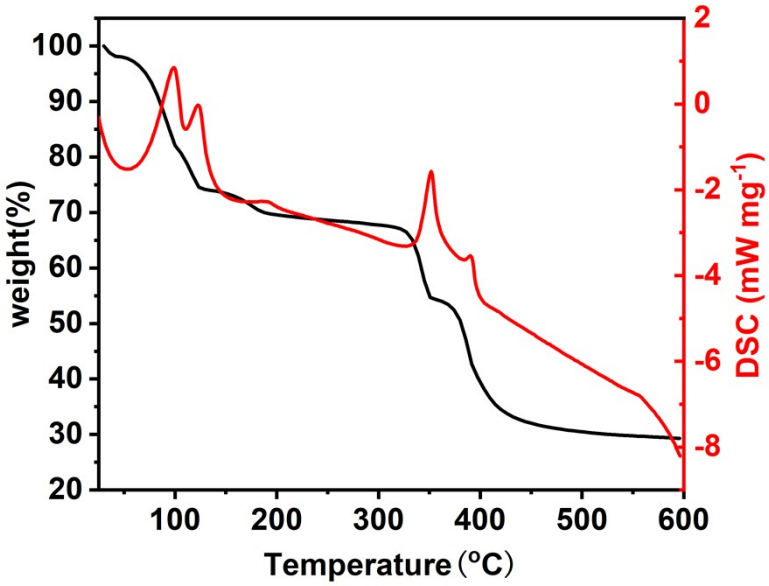

Fig. S3 TG-DSC of **FUT-3**.

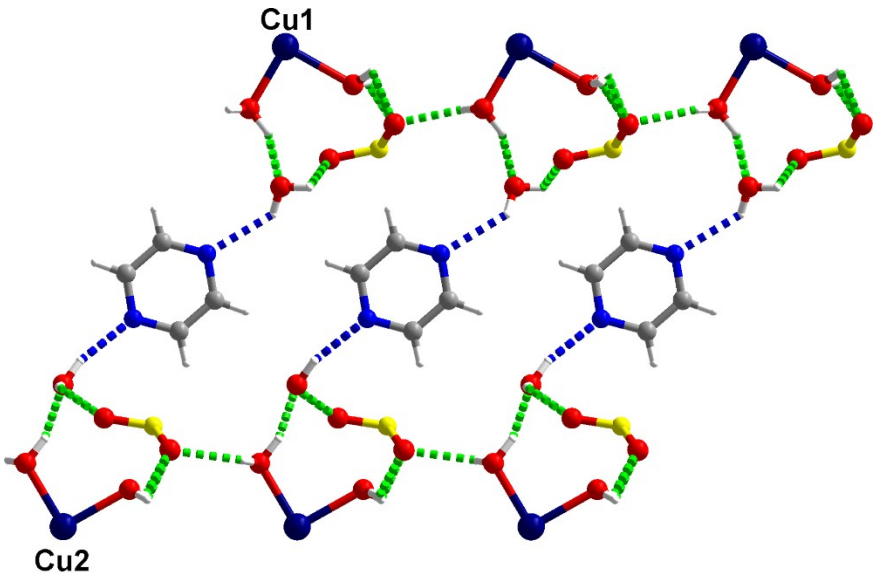

Fig. S4 the hydrogen bonding network between the neighboring chain in **FUT-3** (The figure shows only the sulfonate groups, uncoordinated py and the water molecules.).

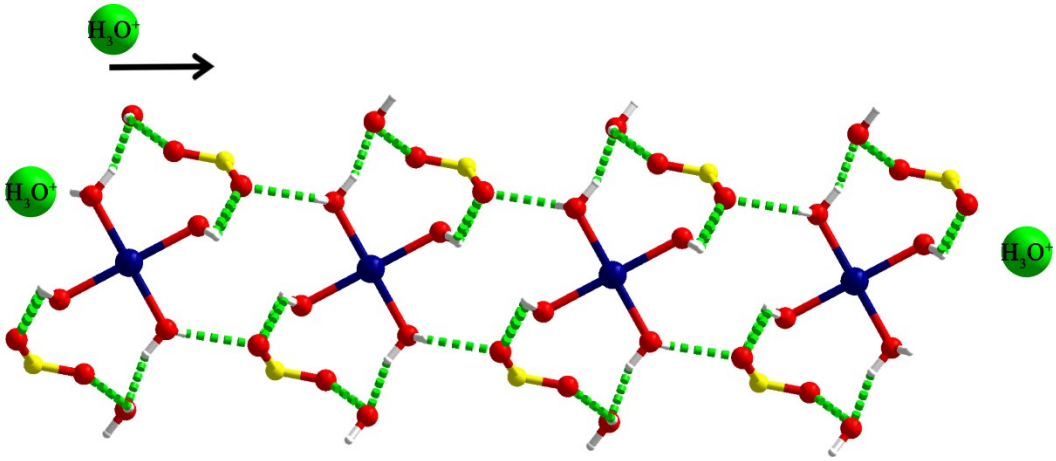

Fig. S5 Schematic representation and possible proton vehicle mechanism of **FUT-3**. The arrows indicate the possible movement of the H_3O^+.

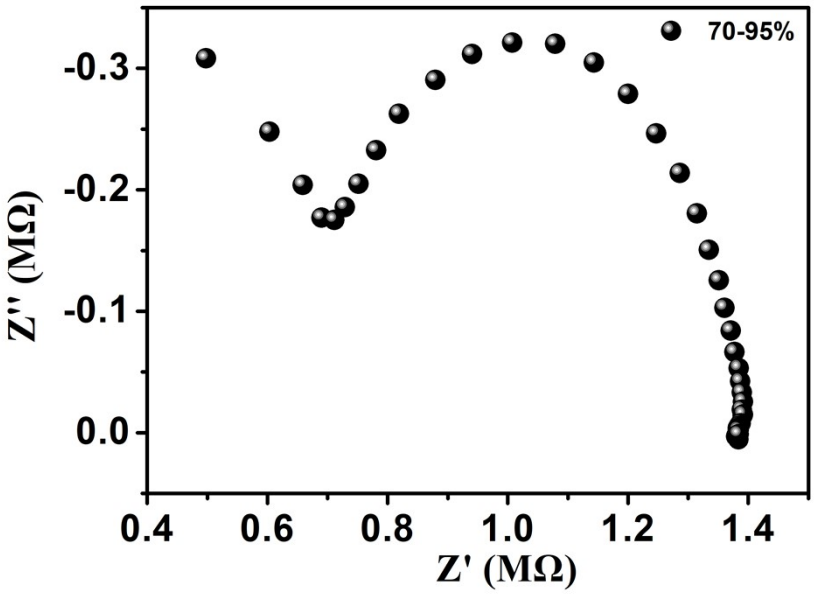

Fig. S6 Nyquist plots of **FUT-3** at 70 °C under 95% RH.

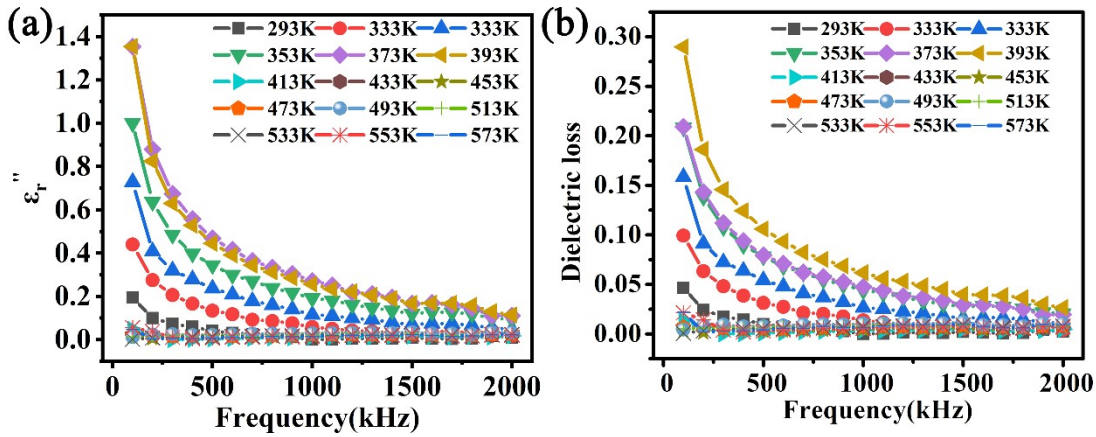

Fig. S7 Frequency dependence of the imaginary part of the relative dielectric constant (ε_r'') (a) and dielectric loss (b) for **FUT-3**.

1 A. V. Dolomanov, L. J. Bourhis, R. J. Gildea, J. A. K. Howard and H. Puschmann, *J. Appl. Crystallogr.,* 2009, **42**, 339–341.

2 L. Palatinus and G. Chapuis, *J. Appl. Crystallogr*., 2007, **40**, 786-790.

3 G. M. Sheldrick, *Acta Crystallogr., Sect. A.,* 2008, **64**, 112-122.